

Development of axially chiral urazole scaffolds for antiplant virus applications against *potato virus Y*

Jiamiao Jin,^a Chengli Mou,^b Juan Zou,^b Xin Xie,^c Chen Wang,^a Tingwei Shen,^a Youlin Deng,^a Benpeng Li,^a Zhichao Jin,^{a*} Xiangyang Li^{a*} and Yonggui Robin Chi^{a,d*}



Abstract

BACKGROUND: *Potato virus Y* (PVY) was first discovered by Smith in 1931 and is currently ranked as the fifth most significant plant virus. It can cause severe damage to plants from the family *Solanaceae*, which results in billions of dollars of economic loss worldwide every year. To discover new antiviral drugs, a class of multifunctional urazole derivatives bearing a stereogenic C–N axis were synthesized with excellent optical purities for antiviral evaluations against PVY.

RESULTS: The absolute configurations of the axially chiral compounds exhibited obvious distinctions in antiviral bioactivities, with several of these enantio-enriched axially chiral molecules showing excellent anti-PVY activities. In particular, compound (R)-9f exhibited remarkable curative activities against PVY with a 50% maximal effective concentration (EC₅₀) of 224.9 µg mL⁻¹, which was better than that of ningnanmycin (NNM), which had an EC₅₀ of 234.0 µg mL⁻¹. And the EC₅₀ value of the protective activities of compound (R)-9f was 462.2 µg mL⁻¹, which was comparable to that of NNM (442.0 µg mL⁻¹). The mechanisms of two enantiomer of the axially chiral compounds 9f were studied by both molecule docking and defensive enzyme activity tests.

CONCLUSION: Mechanistic studies demonstrated that the axially chiral configurations of the compounds played significant roles in the molecule PVY-CP (PVY Coat Protein) interactions and could enhance the activities of the defense enzymes. The (S)-9f showed only one carbon–hydrogen bond and one π –cation interaction between the chiral molecule and the PVY-CP amino acid sites. In contrast, the (R)-enantiomer of 9f exhibited three hydrogen bonding interactions between the carbonyl groups and the PVY-CP active sites of ARG157 and GLN158. The current study provides significant information on the roles that axial chiralities play in plant protection against viruses, which will facilitate the development of novel green pesticides bearing axial chiralities with excellent optical purities. © 2023 Society of Chemical Industry.

Supporting information may be found in the online version of this article.

Keywords: axial chirality; urazole; atropisomer; antiviral; PVY

1 INTRODUCTION

Potato virus Y (PVY) was first discovered by Smith in 1931 and is currently ranked the fifth most significant plant virus.^{1,2} It can cause severe damage to plants from the family *Solanaceae*, which results in billions of dollars of economic loss worldwide every year.^{3–5} For instance, PVY can induce mosaic on the leaves of potato and tobacco. Infections by PVY result in leaf drop in potato plants and deformity, dwarfism and necrosis in tobacco plants. In addition, PVY can be extensively spread by aphids, heredity and mechanical contamination, which makes it one of the most difficult plant pathogens to control in global agricultural production.^{6–10}

Although significant efforts have been made to prevent and cure plant diseases caused by PVY infection, outcomes are far from satisfactory. For instance, the use of resistance cultivars has had a limited effect on alleviating potato leaf/tuber necrotic symptoms caused by PVY infections.^{11,12} Traditional seed-producing procedures can hardly figure out a breed that is prevent from tuber necrosis.¹³ The use of conventional antiplant virus agents

* Correspondence to: Z Jin or X Li or YR Chi, National Key Laboratory of Green Pesticide, Key Laboratory of Green Pesticide and Agricultural Bioengineering, Ministry of Education, Guizhou University, Guiyang, 550025, China. E-mail: zcjin@gzu.edu.cn (Jin), xyl1@gzu.edu.cn (Li) and robinchi@ntu.edu.sg (Chi)

Jiamiao Jin and Chengli Mou contributed equally to this work.

a National Key Laboratory of Green Pesticide, Key Laboratory of Green Pesticide and Agricultural Bioengineering, Ministry of Education, Guizhou University, Guiyang, China

b School of Pharmacy, Guizhou University of Traditional Chinese Medicine, Guiyang, China

c Department of Plant Pathology, College of Agriculture, Guizhou University, Guiyang, China

d School of Chemistry, Chemical Engineering, and Biotechnology, Nanyang Technological University, Singapore, Singapore

such as ribavirin and ningnanmycin (NNM) has had limited field control efficacies against PVY,^{14,15} therefore, the development of effective methods for the control of PVY infection and transmission is of great importance and urgency.

Chemical tools have proven to be effective in plant protection against harmful insects, weeds and various plant pathogens, including bacteria, fungi and viruses.^{16–18} The development and application of green pesticides have made significant contributions to reducing economic loss in world agricultural production. Encouraged by achievements in the development of small molecular green pesticides, we aimed to explore novel chemical structures for the effective control of significant plant viruses such as PVY to facilitate a highly effective plant protection strategy and a clear antiviral mechanism.

It has been well established that the absolute configurations of a chiral molecule play critical roles in their bioactivities in living organisms. Enantiomers of a chiral drug frequently possess different or even controversial bioactive effects in plants, animals and microbes.^{19–24} It has therefore become very important to research and develop enantiomerically pure compounds for agricultural and pharmaceutical applications. However, compared with traditional chiral drugs bearing one or more stereogenic centers, chiral molecules bearing stereogenic axes have been much less explored as pesticides or human drugs.^{25–31} One of the limited examples in the exploration of axial chiralities on pesticide bioactivity was reported by Wen and co-workers in 2019,³² when they systematically studied differences in the bioactivities of the four stereoisomers of metolachlor. Although the axial chiralities in the metolachlor molecules exhibited little impact on their herbicidal activities, they demonstrated substantially different toxicities in aquatic organisms.^{33,34}

There are many reasons why there has been insufficient exploration of axially chiral molecules in pesticide development. One significant factor is the relatively difficult access to enantio-enriched axially chiral compounds. However, recent advances in asymmetric synthesis have provided highly efficient and convenient protocols for achieving axially chiral molecules in an enantioselective fashion, which also provides new opportunities for in-depth investigations into the bioactivities of a diverse range of functional molecules bearing enantio-specific stereogenic axes.^{35–49} Meanwhile, multifunctionalized urazole derivatives have demonstrated excellent biological activity against pathogens, including fungi, bacteria and viruses.^{50–58} As a continuing research program in our laboratory, we are extremely interested in the potential of urazole derivatives bearing axial chiralities in the development of novel pesticides with high antiplant virus efficiency and low nontarget biological risk (Fig. 1).

In this study, we examined the anti-PVY activities of enantio-enriched multisubstituted urazoles bearing a stereogenic axis and a bicyclic fused ring structure (Fig. 2). Enantiomers and racemic mixtures of axially chiral urazole molecules bearing various substituents and substitution patterns were synthesized and systematically studied for their protective, curative and inactivating activities against PVY infections. The absolute configurations of the axially chiral molecules had a significant impact on their antiviral activities. Several of the optically pure compounds showed excellent anti-PVY activities and deserve further exploration as pesticide candidates for plant protection from viral infections.

2 MATERIALS AND METHODS

2.1 Chemicals and instruments

The chemicals were purchased from commercial sources including Energy Chemical, J&K, Aladdin and Bide, and were directly

used without further purification (China). The ¹H NMR spectra of the known axially chiral urazole compounds were collected on a Bruker Ascend 400 (400 MHz) spectrometer (Bruker, Germany). The enantiomeric ratios of the axially chiral compounds were obtained via ultrahigh-performance liquid chromatography (UPLC) (waters, USA) analysis on a Waters system with an Empower 3 system controller, Waters UPLC H-Class (waters, USA) and Shimadzu Prominence LC-20A (Shimadzu, Japan), and Waters Acquity UPLC PDA (Photodiode Array) detector. Chiralcel brand chiral columns from Daicel Chemical Industries, models IA-U, IB-U, IE-U and AD-3, were used in the 3.0 × 100 mm size.

2.2 General procedures for the preparation of intermediates 4a–4s

To a stirred solution of aryl iodide **1** (5.0 mmol) and 3,3-diethoxyprop-1-yne **2** (7.0 mmol) in tetrahydrofuran (THF; 15 mL) was added triethylamine (3.0 mL), palladium catalyst Pd(PPh₃)₂Cl₂ (0.5 mmol) and copper(I) iodide (0.5 mmol). The reaction mixture was stirred for 4 h at 25 °C under air conditions. The volatiles were removed under reduced pressure and the residue was suspended in water (15 mL). After extraction with dichloromethane (DCM; 3 × 50 mL), the organic layers were combined, dried with Na₂SO₄ and concentrated *in vacuo*. The residue was purified through column chromatography to give the pure intermediate **3**, which was then hydrolyzed in water (10 mL) and acetone (10 mL) in the presence of aqueous HCl (5% in water, 15 mL). After stirring at room temperature for 12 h, the reaction mixture was extracted with DCM (3 × 20 mL). The organic extracts were combined, dried, concentrated and purified via column chromatography to yield the pure ynal intermediate **4**.

2.3 General procedures for the preparation of intermediates 8a–8c

Triphosgene (10.0 mmol) was dissolved in dry DCM (50 mL) at 0 °C and Et₃N (3 mL) was added with stirring. After 5 min, a solution of the aromatic amine **5** (10.0 mmol) in dry DCM (50 mL) was slowly added to the reaction mixture at 0 °C and the reaction system was stirred at room temperature for 12 h. After removing the volatiles under reduced pressure, the crude intermediate **6** was afforded as a yellow solid and directly used in the next step.

To the solution of the crude intermediate **6** in THF (50 mL) was added methyl carbazate (10 mmol) and the reaction mixture was stirred at room temperature. After the reaction was completed (monitored by thin-layer chromatography, generally within 15 min), the solvent was removed under reduced pressure. The residue was suspended in water and filtered to give the crude intermediate **7**, which was directly used in the next step.

The homogeneous solution of the crude intermediate **7** in aqueous potassium hydroxide (4 M, 50 mL) was heated to reflux with stirring for 5 h. The reaction solution was cooled to room temperature and carefully acidified by aqueous HCl (1 N) to pH 2. The suspension was filtered and the solid was collected and washed with cold water. The solid was then dissolved in ethyl acetate and dried over Na₂SO₄. After filtration the solvent was removed under vacuum and the pure intermediate **8** was afforded as a white solid.

2.4 General procedures for the preparation of the axially chiral urazole products (S)-9a–(S)-9u

To a round-bottomed flask equipped with a magnetic stirring bar was sequentially added the chiral NHC (N-Heterocyclic carbene) pre-catalyst **A** (0.2 mmol, 20 mol%), Na₂CO₃ (0.2 mmol, 20 mol

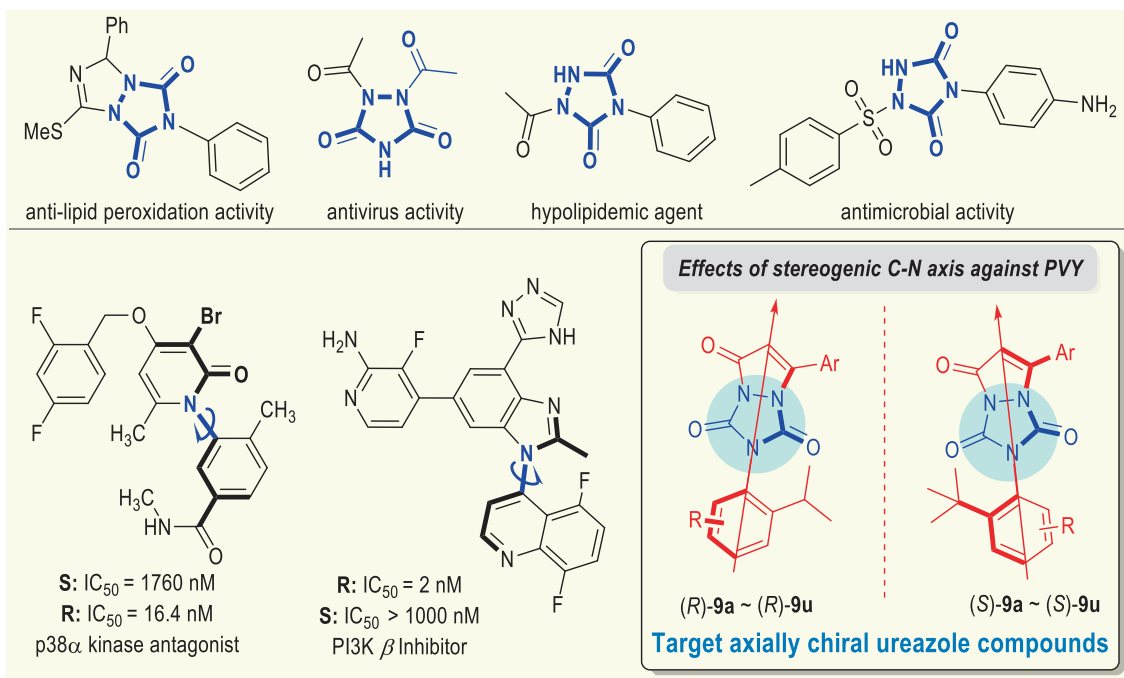


Figure 1. Design of target compounds.

%), the oxidant **B** (1.5 mmol, 150 mol%) and intermediates **8** (1.0 mmol). The solid mixture was dissolved in dry THF (10 mL), sealed and cooled to -20°C . Then a solution of the intermediates **4** (1.5 mmol) in anhydrous THF (10 mL) was added via syringe and the reaction mixture was stirred at -20°C for 24 h. The reaction mixture was concentrated under vacuum and the residue was purified via column chromatography on silica gel using hexane/EtOAc (3:1, v/v) as eluent to afford the pure chiral products (**S**)-**9a**–(**S**)-**9u**. An additional recrystallization step was sometimes needed to obtain an improved optical purity.

2.5 General procedures for the preparation of the axially chiral urazole products (*R*)-**9a**–(*R*)-**9u**

To a round-bottomed flask equipped with a magnetic stirring bar was sequentially added the chiral NHC pre-catalyst *ent*-**A** (0.2 mmol, 20 mol%), Na_2CO_3 (0.2 mmol, 20 mol%), the oxidant **B** (1.5 mmol, 150 mol%) and the intermediates **8** (1.0 mmol). The solid mixture was dissolved in dry THF (10 mL), sealed and cooled to -20°C . Then a solution of the intermediates **4** (1.5 mmol) in anhydrous THF (10 mL) was added via syringe and the reaction mixture was stirred at -20°C for 24 h. The reaction mixture was concentrated under vacuum and the residue was purified via column chromatography on silica gel using hexane/EtOAc (3:1, v/v) as eluent to afford the pure chiral products (*R*)-**9a**–(*R*)-**9u**. An additional recrystallization step was sometimes needed to obtain an improved optical purity.

2.6 General procedures for the preparation of the axially chiral urazole products (*rac*)-**9a**–(*rac*)-**9u**

To a round-bottomed flask equipped with a magnetic stirring bar was sequentially added the chiral NHC pre-catalyst **A** (0.1 mmol, 10 mol%), the chiral NHC pre-catalyst *ent*-**A** (0.1 mmol, 10 mol %), Na_2CO_3 (0.2 mmol, 20 mol%), the oxidant **B** (1.5 mmol, 150 mol%) and the intermediates **8** (1.0 mmol). The solid mixture was dissolved in dry THF (10 mL), sealed and cooled to -20°C .

Then a solution of the intermediates **4** (1.5 mmol) in anhydrous THF (10 mL) was added via syringe and the reaction mixture was stirred at -20°C for 24 h. The reaction mixture was concentrated under vacuum and the residue was purified via column chromatography on silica gel using hexane/EtOAc (3:1, v/v) as eluent to afford the pure chiral products (*rac*)-**9a**–(*rac*)-**9u**.

2-(2-(tert-butyl)phenyl)-7-phenyl-1*H*,5*H*-pyrazolo[1,2-*a*][1,2,4]triazole-1,3,5(2*H*)-trione (**9a**): ^1H NMR (400 MHz, CDCl_3) δ 7.84–7.82 (m, 2H), 7.64–7.58 (m, 2H), 7.52 (dd, $J = 8.3, 6.7$ Hz, 2H), 7.49–7.44 (m, 1H), 7.31 (td, $J = 7.6, 1.5$ Hz, 1H), 7.09 (dd, $J = 7.8, 1.5$ Hz, 1H), 6.03 (s, 1H), 1.41 (s, 9H).

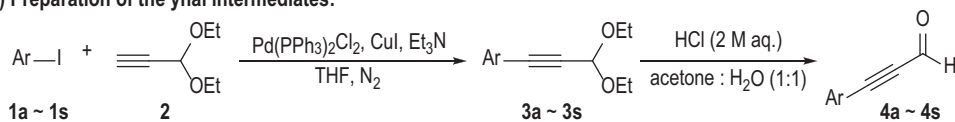
2.7 Antiviral activity evaluation

The PVY virus was obtained from the infected *Nicotiana tabacum* K326 leaves according to reported procedures. The antiviral activities of the axially chiral compounds against PVY were evaluated through the half-leaf method on *Chenopodium amaranticolor* plants from the same period. The EC_{50} (50% maximal effective concentration) values were calculated based on the antiviral activities of the same chiral compounds at concentrations of 500, 250, 125, 62.5 and 31.25 mg L^{-1} . The commercial antiviral drug NNM was selected as the control agent. The lesions were counted and recorded after 3–4 days. All the antiviral activity tests were repeated three times.

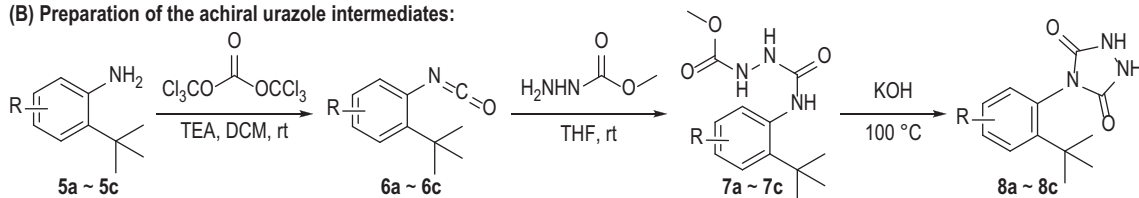
2.7.1 Curative effects of the axially chiral urazole compounds

After sprinkling evenly with the silicon carbide, the leaves of *Chenopodium amaranticolor* plants were rubbed lightly with a brush that had been carefully dipped in PVY solution. After inoculation for 1.5 h, the leaves were washed with water. The solutions of the chiral compounds were prepared using dimethyl sulfoxide (DMSO) and 2.0% Tween 80 as the solvent. The chiral compound solutions were transferred onto the right half of the leaves with a brush, while the mixture of the DMSO and 2.0% Tween 80 was transferred onto the left half of the leaves as the blank control. The lesions were counted and recorded after 3–4 days.

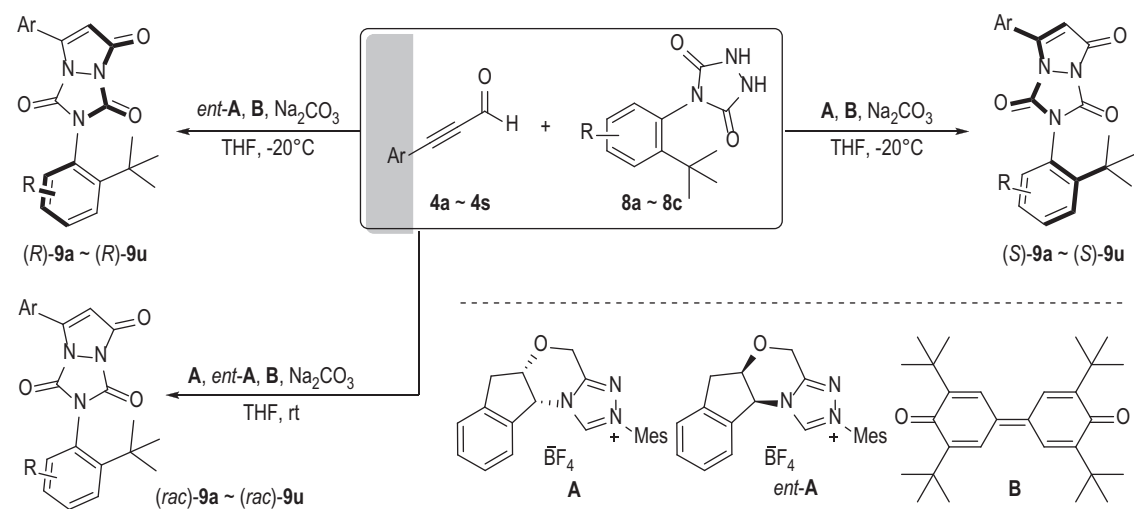
(A) Preparation of the ynal intermediates:



(B) Preparation of the achiral urazole intermediates:



(C) Preparation of the target axially chiral urazole products:



(S)-9a, (R)-9a, (rac)-9a: R = H, Ar = Ph
(S)-9b, (R)-9b, (rac)-9b: R = H, Ar = 2-CH₃-Ph
(S)-9c, (R)-9c, (rac)-9c: R = H, Ar = 3-CH₃-Ph
(S)-9d, (R)-9d, (rac)-9d: R = H, Ar = 4-CH₃-Ph
(S)-9e, (R)-9e, (rac)-9e: R = H, Ar = 2-Cl-Ph
(S)-9f, (R)-9f, (rac)-9f: R = H, Ar = 3-Cl-Ph
(S)-9g, (R)-9g, (rac)-9g: R = H, Ar = 4-Cl-Ph
(S)-9h, (R)-9h, (rac)-9h: R = H, Ar = 2-F-Ph
(S)-9i, (R)-9i, (rac)-9i: R = H, Ar = 3-F-Ph
(S)-9j, (R)-9j, (rac)-9j: R = H, Ar = 4-F-Ph
(S)-9k, (R)-9k, (rac)-9k: R = H, Ar = 3-OCH₃-Ph

(S)-9l, (R)-9l, (rac)-9l: R = H, Ar = 4-OCH₃-Ph
(S)-9m, (R)-9m, (rac)-9m: R = H, Ar = 2-NO₂-Ph
(S)-9n, (R)-9n, (rac)-9n: R = H, Ar = 3-NO₂-Ph
(S)-9o, (R)-9o, (rac)-9o: R = H, Ar = 4-NO₂-Ph
(S)-9p, (R)-9p, (rac)-9p: R = H, Ar = 2-CN-Ph
(S)-9q, (R)-9q, (rac)-9q: R = H, Ar = 4-acetylphenyl
(S)-9r, (R)-9r, (rac)-9r: R = H, Ar = naphthalen-1-yl
(S)-9s, (R)-9s, (rac)-9s: R = H, Ar = thiophen-2-yl
(S)-9t, (R)-9t, (rac)-9t: R = 4-Cl, Ar = Ph
(S)-9u, (R)-9u, (rac)-9u: R = 4-Br, Ar = Ph

Figure 2. Synthesis of the axially chiral urazole products 9a to 9u.

2.7.2 Protective effects of the axially chiral urazole compounds

Solutions of the axially chiral compounds in the mixed solvent of DMSO and 2% Tween 80 were evenly transferred onto the right side of leaves of *Chenopodium amaranticolor* plants with a brush. After 24 h, silicon carbide was evenly sprinkled onto the leaves and the PVY solution was then carefully transferred onto the leaves with a brush. After 1.5 h, the leaves were washed with water, and the number of lesions was counted and recorded after 3–4 days.

2.7.3 Inactivating effects of the axially chiral urazole compounds

To solutions of the axially chiral compounds in a mixed solvent of DMSO and 2% Tween 80 was added the PVY solution in equal volumes. The mixtures were cooled at 0 °C for 30 min. The cooled

solutions were carefully transferred onto the right side of the leaves and the left side of the leaves was rubbed with PVY solution in a mixed solvent of DMSO and 2% Tween 80 as the control experiment. After 1.5 h, the leaves were washed with water, and the number of lesions was counted and recorded after 3–4 days.

2.8 Agrobacterium infection of PVY-GFP on *N. benthamiana* L. leaves

The leaves of *N. benthamiana* L. were injected with an inoculum of PVY-green fluorescent protein (GFP) via a syringe (without a needle). After 24 h, a solution of the axially chiral compound in the mixed solvent consisting of DMSO and 2% Tween 80 was sprayed onto the infected leaves. After an additional 48 h, the solution of the axially chiral compound was sprayed onto the leaves again. A solution of NNM was used as the positive control. After 9 days,

the expression of GFP on the host plants was examined under ultraviolet irradiation.

2.9 Defense enzyme activity evaluation

Tobaccos were treated with the axially chiral compounds (**S**)-**9f** and (**R**)-**9f** at the six-leaf stage. NNM was used as the positive control. DMSO/2% Tween 80 solutions of compounds (**S**)-**9f**, (**R**)-**9f** and NNM (500 mg L⁻¹) were evenly rubbed onto the tobacco leaves. After 24 h, the treated leaves were evenly sprinkled with silicon carbide and then rubbed lightly with a brush that had been carefully dipped into the PVY solution. The tobacco leaves were collected on the first, third, fifth, and seventh days and kept at -80 °C. Then 0.1 g of each of the leaf samples was frozen with liquid nitrogen, grinded and then treated with defensive enzyme test kits purchased from Suzhou Comin Biotechnology Co., Ltd, China (This manufacturer is located in Suzhou, Jiangsu Province). The activities of catalase (CAT), peroxidase (POD), superoxide dismutase (SOD) and phenylalanine ammonia-lyase (PAL) were examined according to reported procedures. All the defense enzyme activity tests were repeated three times.

2.10 Molecule docking

The three-dimensional (3D) structures of the axially chiral compounds (**S**)-**9f**, (**R**)-**9f**, (**S**)-**9h** and (**R**)-**9h** were constructed using Discovery Studio 2020 Client software and optimized through the MM2 project to obtain the conformation with the lowest energy. The 3D structure of PVY-CP was obtained from the Protein Data Bank (PDB) database and downloaded at <https://www.rcsb.org/>. The elimination of water, prediction of the docking pockets, hydrogenation and conformation optimization of the PVY-CP structure were carried out using Discovery Studio 2020 Client software. The optimized PVY-CP structure was identified as the receptor and exported as a pdbqt file. The docking program was

implemented by Autodock vina 1.1.2, and BIOVIA Discovery Studio 2020 was used to process the docking result and export a visible figure.

3 RESULTS AND DISCUSSION

3.1 Chemistry

The aryl iodide **1** reacted with 3,3-diethoxyprop-1-yne **2** under catalysis with Pd(PPh₃)₂Cl₂ and Cul to give the aryl alkyne acetal intermediate **3**, which was then hydrolyzed under acidic conditions to give the ynal intermediate **4** (Fig. 2). Meanwhile, 2-*tert*-butylaniline **5** reacted with triphosgene to give the isocyanate intermediate **6**, which was attacked by methyl hydrazinecarboxylate to give the urea intermediate **7**. An intramolecular ester amidation process with **7** afforded the urazine intermediate **8**.

The axially chiral product (**S**)-**9** was obtained from the atropoe-nantioselective [3 + 2] cycloaddition reaction between intermediates **4** and **8** under catalysis with the chiral NHC catalyst **A** in the presence of a stoichiometric amount of the external oxidant **B**. Similarly, the axially chiral product (**R**)-**9** and the racemic product (*rac*)-**9** were obtained from the reaction between **4** and **8** using *ent*-**A** and racemic **A**, respectively, as the reaction catalyst under the same reaction conditions.

Mechanistically, the deprotonated free chiral NHC catalyst reacts with the ynal **4a** under oxidative conditions to give the acylazolium intermediate **I** (Fig. 3). Then the chiral intermediate **I** reacts with the urazole substrate **8a** via a reversible atropoe-nantioselective aza-Michael addition reaction to give the diastereo-isomeric adducts **II** and **III**. Adduct **III** is thermodynamically unstable and can go back to intermediate **I** and urazole **2a** due to steric reasons. Therefore, the stereo-specific intermediate **IV** is afforded as the major intermediate after a dynamic kinetic resolution process from the adducts **II** and **III**. Finally, a lactam formation process within

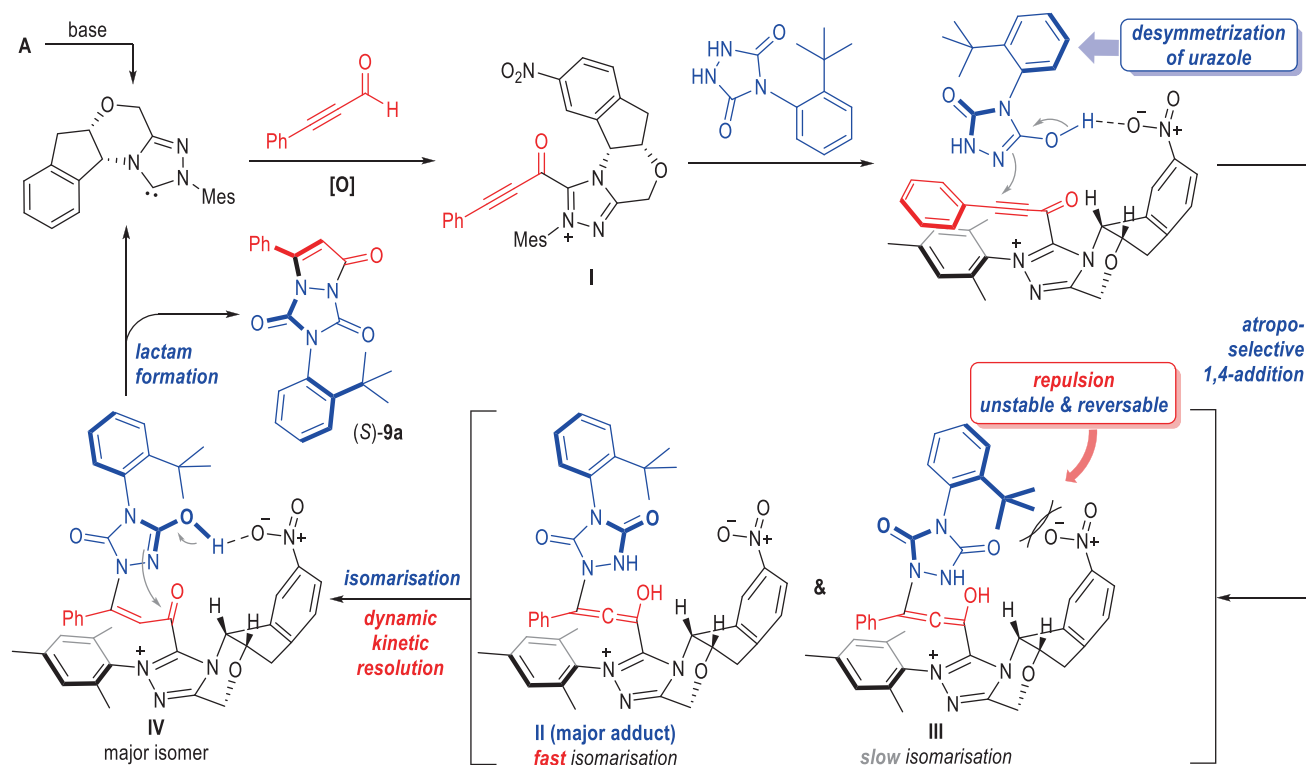
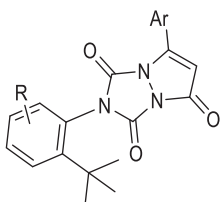


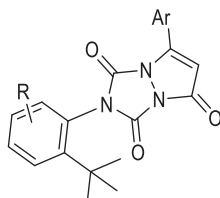
Figure 3. Proposed reaction mechanism for the formation of (**S**)-**9a**.

Table 1. Antiviral activities of compounds against PVY^a



Compound	R	Ar	EE (%)	Curative activity (%)	Protective activity (%)	Inactivating activity (%)
(S)-9a	H	Ph	94	44.36 ± 1.45	32.00 ± 0.91	64.71 ± 4.07
(R)-9a	H	Ph	96	41.45 ± 6.69	6.93 ± 2.85	56.04 ± 4.79
(rac)-9a	H	Ph	0	48.55 ± 2.44	27.75 ± 1.85	61.73 ± 3.83
(S)-9b	H	2-CH ₃ -Ph	94	48.80 ± 4.29	48.80 ± 9.96	41.29 ± 2.80
(R)-9b	H	2-CH ₃ -Ph	92	49.94 ± 3.11	54.84 ± 3.83	34.70 ± 4.26
(rac)-9b	H	2-CH ₃ -Ph	0	49.83 ± 8.52	41.73 ± 3.30	62.45 ± 3.69
(S)-9c	H	3-CH ₃ -Ph	90	31.52 ± 2.11	46.53 ± 4.55	60.96 ± 6.21
(R)-9c	H	3-CH ₃ -Ph	94	58.71 ± 6.33	51.25 ± 3.42	60.55 ± 4.93
(rac)-9c	H	3-CH ₃ -Ph	0	47.01 ± 2.70	69.63 ± 1.27	62.64 ± 0.57
(S)-9d	H	4-CH ₃ -Ph	90	18.89 ± 0.54	49.70 ± 1.40	60.24 ± 0.68
(R)-9d	H	4-CH ₃ -Ph	90	34.17 ± 5.11	38.93 ± 3.89	49.14 ± 5.17
(rac)-9d	H	4-CH ₃ -Ph	0	24.38 ± 3.85	38.22 ± 3.10	62.30 ± 5.94
(S)-9e	H	2-Cl-Ph	94	47.88 ± 4.18	47.65 ± 5.07	48.60 ± 5.88
(R)-9e	H	2-Cl-Ph	90	37.94 ± 1.82	44.63 ± 4.90	33.05 ± 0.86
(rac)-9e	H	2-Cl-Ph	0	42.32 ± 8.19	52.39 ± 4.14	36.54 ± 1.94
(S)-9f	H	3-Cl-Ph	96	30.53 ± 4.07	39.20 ± 4.69	44.20 ± 5.95
(R)-9f	H	3-Cl-Ph	99	50.47 ± 6.45	51.91 ± 2.88	54.73 ± 2.40
(rac)-9f	H	3-Cl-Ph	0	49.58 ± 4.17	57.09 ± 3.40	51.11 ± 3.62
(S)-9g	H	4-Cl-Ph	99	34.47 ± 2.37	50.18 ± 3.90	50.45 ± 1.06
(R)-9g	H	4-Cl-Ph	99	58.40 ± 2.53	70.33 ± 1.83	43.86 ± 4.56
(rac)-9g	H	4-Cl-Ph	0	37.07 ± 2.11	51.74 ± 7.58	49.64 ± 5.07
(S)-9h	H	2-F-Ph	84	43.65 ± 0.92	53.48 ± 3.51	50.38 ± 2.25
(R)-9h	H	2-F-Ph	78	37.19 ± 7.95	52.53 ± 2.48	26.11 ± 2.83
(rac)-9h	H	2-F-Ph	0	47.88 ± 5.21	36.77 ± 5.11	47.90 ± 3.30
(S)-9i	H	3-F-Ph	99	37.21 ± 1.67	53.48 ± 3.51	60.66 ± 2.14
(R)-9i	H	3-F-Ph	90	37.52 ± 6.44	52.53 ± 2.48	66.83 ± 3.74
(rac)-9i	H	3-F-Ph	0	26.38 ± 1.63	55.18 ± 3.79	51.61 ± 5.05
(S)-9j	H	4-F-Ph	99	21.88 ± 3.68	46.39 ± 6.05	59.24 ± 2.29
(R)-9j	H	4-F-Ph	74	23.18 ± 2.17	44.68 ± 3.69	51.65 ± 4.23
(rac)-9j	H	4-F-Ph	0	12.42 ± 2.63	46.61 ± 5.93	50.29 ± 2.24
(S)-9k	H	3-OCH ₃ -Ph	80	47.07 ± 3.19	46.60 ± 3.49	47.10 ± 3.89
(R)-9k	H	3-OCH ₃ -Ph	84	42.33 ± 3.49	42.33 ± 3.49	57.65 ± 2.95
(rac)-9k	H	3-OCH ₃ -Ph	0	43.07 ± 3.57	43.07 ± 3.57	61.56 ± 3.30
(S)-9l	H	4-OCH ₃ -Ph	90	54.38 ± 4.92	45.58 ± 2.30	48.33 ± 2.13
(R)-9l	H	4-OCH ₃ -Ph	98	28.64 ± 2.55	42.52 ± 5.15	66.20 ± 3.61
(rac)-9l	H	4-OCH ₃ -Ph	0	49.95 ± 4.61	60.48 ± 4.89	58.29 ± 5.50
(S)-9m	H	2-NO ₂ -Ph	88	48.17 ± 4.53	36.37 ± 5.95	68.58 ± 2.96
(R)-9m	H	2-NO ₂ -Ph	98	26.85 ± 2.31	52.98 ± 3.64	58.72 ± 1.50
(rac)-9m	H	2-NO ₂ -Ph	0	42.53 ± 3.26	50.54 ± 2.39	61.18 ± 3.94
(S)-9n	H	3-NO ₂ -Ph	99	42.82 ± 3.23	55.74 ± 4.11	71.95 ± 0.43
(R)-9n	H	3-NO ₂ -Ph	94	36.27 ± 3.81	45.43 ± 7.56	74.01 ± 1.44
(rac)-9n	H	3-NO ₂ -Ph	0	19.28 ± 4.61	45.13 ± 2.33	50.15 ± 0.38
(S)-9o	H	4-NO ₂ -Ph	76	50.51 ± 2.59	42.81 ± 22.90	61.32 ± 6.13
(R)-9o	H	4-NO ₂ -Ph	70	33.25 ± 3.90	47.06 ± 4.04	68.65 ± 2.37
(rac)-9o	H	4-NO ₂ -Ph	0	37.54 ± 1.10	41.22 ± 5.38	68.65 ± 2.37
(S)-9p	H	2-CN-Ph	80	52.35 ± 2.80	52.85 ± 2.79	53.59 ± 4.89
(R)-9p	H	2-CN-Ph	68	25.05 ± 1.51	16.80 ± 3.16	58.88 ± 2.44
(rac)-9p	H	2-CN-Ph	0	48.69 ± 11.56	46.64 ± 3.91	59.57 ± 2.56
(S)-9q	H	4-acetylphenyl	96	24.04 ± 4.50	46.15 ± 3.29	63.00 ± 1.32
(R)-9q	H	4-acetylphenyl	90	12.01 ± 3.97	30.95 ± 4.89	65.97 ± 4.49

Table 1. Continued



Compound	R	Ar	EE (%)	Curative activity (%)	Protective activity (%)	Inactivating activity (%)
(rac)-9q	H	4-acetylphenyl	0	23.72 ± 4.25	33.00 ± 3.20	66.53 ± 5.80
(S)-9r	H	naphthalen-1-yl	96	42.60 ± 5.57	52.71 ± 6.50	69.92 ± 3.66
(R)-9r	H	naphthalen-1-yl	96	29.10 ± 4.08	51.89 ± 5.24	54.73 ± 5.71
(rac)-9r	H	naphthalen-1-yl	0	27.29 ± 8.13	28.51 ± 4.98	70.19 ± 4.78
(S)-9s	H	thiophen-2-yl	90	43.62 ± 3.11	33.73 ± 4.53	58.40 ± 4.27
(R)-9s	H	thiophen-2-yl	90	24.53 ± 4.82	47.58 ± 6.27	56.12 ± 4.77
(rac)-9s	H	thiophen-2-yl	0	50.52 ± 3.19	32.80 ± 4.03	50.88 ± 1.01
(S)-9t	4-Cl	Ph	88	39.19 ± 8.81	44.92 ± 1.06	67.12 ± 4.67
(R)-9t	4-Cl	Ph	92	34.39 ± 4.21	57.05 ± 4.47	55.28 ± 4.17
(rac)-9t	4-Cl	Ph	0	56.11 ± 0.64	43.40 ± 8.48	73.99 ± 2.91
(S)-9u	4-Br	Ph	99	38.07 ± 1.75	48.61 ± 3.31	58.47 ± 3.19
(R)-9u	4-Br	Ph	999	36.24 ± 0.96	41.68 ± 3.20	63.93 ± 4.70
(rac)-9u	4-Br	Ph	0	26.50 ± 2.47	53.66 ± 0.94	72.68 ± 4.23
NNM ^b	–	–	–	48.73 ± 0.88	53.27 ± 4.52	79.23 ± 4.93

Abbreviations: PVY, potato virus Y; NNM, ningnanmycin; EE, Enantiomeric Excess.

^a Average of three replicates.^b Commercial antiviral agent ningnanmycin as positive control.Table 2. EC₅₀ of active title compounds against PVY

Compound	Curative effect			Protective effect		
	Regression equation	R ²	EC ₅₀ (μg mL ⁻¹)	Regression equation	R ²	EC ₅₀ (μg mL ⁻¹)
(R)-9c	y = 1.039x + 2.59	0.99	208.4	y = 0.591x + 3.52	0.97	321.1
(R)-9 f	y = 0.757x + 3.22	0.97	224.9	y = 0.555x + 3.52	0.96	462.2
(R)-9 g	y = 1.04x + 2.47	0.97	268.8	y = 0.949x + 2.63	0.97	315.7
NNM	y = 0.753x + 3.22	0.98	234.0	y = 0.682x + 3.20	0.98	442.0

Abbreviations: EC₅₀, 50% maximal effective concentration; PVY, potato virus Y; NNM, ningnanmycin.

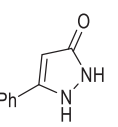
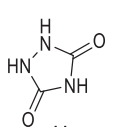
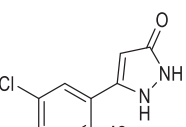
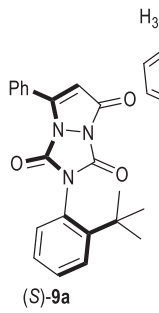
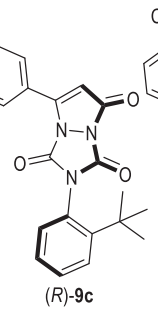
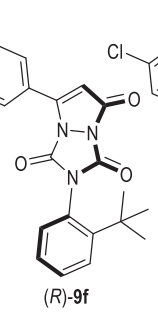
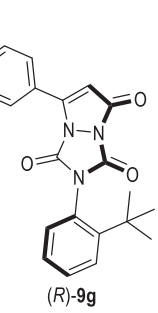
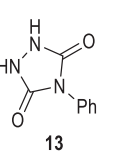
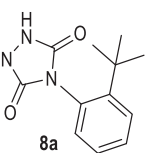
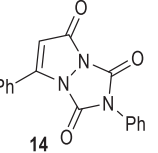
intermediate **IV** affords the target axially chiral product (**S**)-**9a** with elimination of the free NHC catalyst.

3.2 Antiviral activity

Solutions of the enantio-enriched axially chiral compounds (**S**)-**9a–9u**, (**R**)-**9a–9u** and their racemic mixtures in DMSO/2% Tween 80 were prepared at a concentration of 500 μg mL⁻¹. The stereochemistry of most of the axially chiral molecules exhibited obvious impacts on their antiviral bioactivities (Table 1). For instance, the optically enriched (**R**)-**9c**, (**R**)-**9f** and (**R**)-**9g** showed much better curative activities against PVY than their enantiomers or their racemic mixtures, with inactivation rates of 59%, 50% and 58%, respectively, which are better than the positive control with NNM (inactivation rate 49%). Several axially chiral compounds **9** bearing (**S**)-configurations also exhibited better antiviral

activities against PVY than their (**R**)-enantiomers or racemic mixtures, such as (**S**)-**9l**, (**S**)-**9o** and (**S**)-**9p**, with inactivation rates of 54%, 51% and 52%, respectively. Interestingly, the racemic mixtures of the axially chiral compounds **9s** and **9t** showed excellent curative antiviral activities of 51% and 56%, respectively, which were much better than any of their enantio-pure isomers or the positive control of NNM. Three of the optically pure compounds bearing (**R**)-configurations, (**R**)-**9b**, (**R**)-**9g** and (**R**)-**9t**, exhibited excellent protective antiviral activities against PVY with inhibition rates of 55%, 70% and 57%, respectively, which were superior to their (**S**)-enantiomers, racemic mixtures or the positive control of NNM. In addition, three racemic mixtures of the axially compounds also showed better protective activities against PVY than NNM or their enantio-enriched stereoisomers, with inhibition rates of 57% (**9f**), 60% (**9l**) and 54% (**9u**), respectively. In contrast,

Table 3. Comparison of the antiviral activities of the chiral compounds and the molecular fragments

						
						
10	11	12	13	8a	14	

Compound	Curative activity (%)	Protective activity (%)	Compound	Curative activity (%)	Protective activity (%)
10	17.26 ± 1.59	22.64 ± 3.20	(S)-9c	31.52 ± 2.11	46.53 ± 4.55
11	24.68 ± 1.73	23.50 ± 4.99	(R)-9c	58.71 ± 6.33	51.25 ± 3.42
12	35.31 ± 3.34	26.79 ± 5.37	(rac)-9c	47.01 ± 2.70	69.63 ± 1.27
13	32.79 ± 0.66	31.50 ± 5.74	(S)-9f	30.53 ± 4.07	39.20 ± 4.69
8a	18.22 ± 5.62	24.72 ± 1.79	(R)-9f	50.47 ± 6.45	51.91 ± 2.88
14	26.63 ± 5.21	23.34 ± 4.66	(rac)-9f	49.58 ± 4.17	57.09 ± 3.40
(S)-9a	44.36 ± 1.45	32.00 ± 0.91	(S)-9g	34.47 ± 2.37	50.18 ± 3.90
(R)-9a	41.45 ± 6.69	6.93 ± 2.85	(R)-9g	58.40 ± 2.53	70.33 ± 1.83
(rac)-9a	48.55 ± 2.44	27.75 ± 1.85	(rac)-9g	37.07 ± 2.11	51.74 ± 7.58

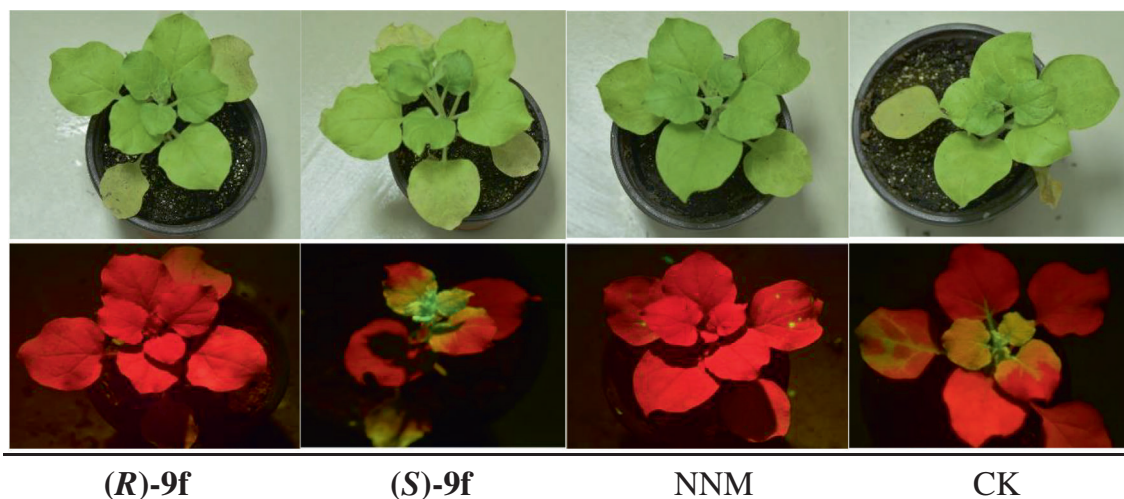


Figure 4. The result of the expression of PVY-GFP.

only one (*S*)-enantiomer (**9n**) showed good protective activity (56%) that was superior to its enantiomer, racemate or the NNM. Disappointingly, none of the axially chiral molecules showed superior inactivating activities against PVY to NNM. However, the racemates of compounds **9t** and **9u** showed comparative inhibition rates to NNM, and both of the enantiomers of the axially chiral **9n** showed better inactivation activities than its racemic mixture and were also comparative to NNM.

Based on the comprehensive antiviral activities of the axially chiral molecules, we can identify that three optically pure molecules, (*R*)-**9c**, (*R*)-**9f** and (*R*)-**9g**, possessed both good curative and protective activities against PVY, therefore the EC_{50} values of these compounds were calculated in comparison with the commercial antiviral drug NNM (Table 2). The EC_{50} values of (*R*)-**9c** and (*R*)-**9f** were 208.4

and 224.9 $\mu\text{g mL}^{-1}$, respectively, which is better than that for NNM, with EC_{50} values of 234.0 $\mu\text{g mL}^{-1}$. The EC_{50} value of (*R*)-**9g** in the curative effect was 268.8 $\mu\text{g mL}^{-1}$, which is slightly inferior to that of NNM. The EC_{50} value of (*R*)-**9c** and (*R*)-**9g** in the protective effects were 321.1 and 315.7 $\mu\text{g mL}^{-1}$, respectively, which is superior to that of NNM (442.0 $\mu\text{g mL}^{-1}$). The EC_{50} value of (*R*)-**9f** was 462.2 $\mu\text{g mL}^{-1}$, which is comparable to that of NNM.

3.3 Structure–activity relationships

To examine the structure–activity relationship (SAR) of the axially chiral antiviral molecules, each fragment of these compounds was synthesized and evaluated in anti-PVY activities (Table 3). Both the dihydropyrazolone **10** and the urazole **11** fragments showed poor activities against PVY. Introducing substituents on the

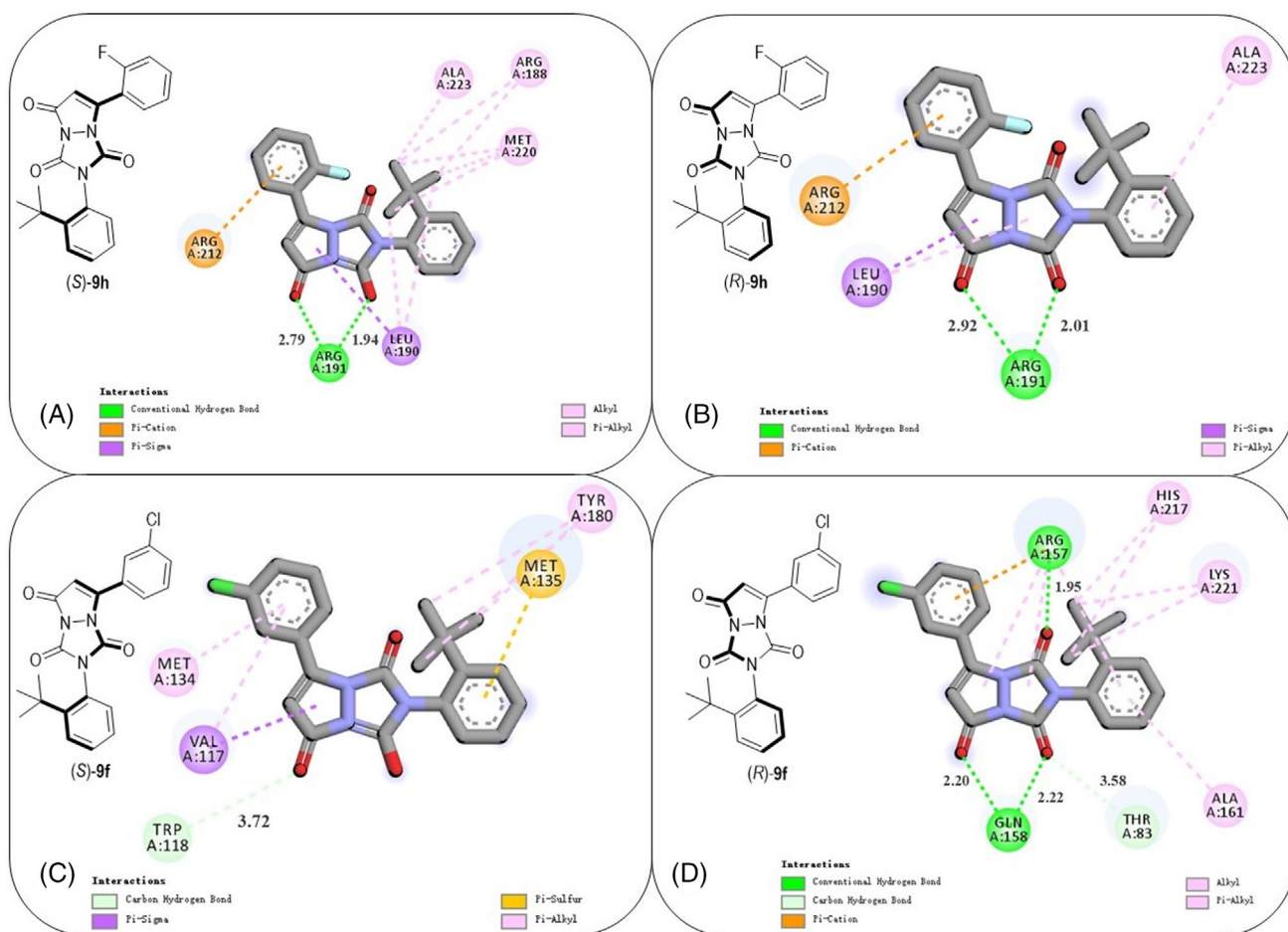


Figure 5. Molecule docking between target compounds and PVY-CP. (A) Autodocking of compound (S)-9h, (B) autodocking of compound (R)-9h, (C) autodocking of compound (S)-9f and (D) autodocking of compound (R)-9f.

phenyl group of the dihydropyrazolone fragment (e.g. **12**) slightly improved the antiviral activities. Although the N-phenyl urazole fragment **13** showed promising antiviral activities, the starting material **8a** bearing a bulky N-substituent exhibited poor bioactivity. Fusing fragments **10** and **11** resulted in little improvement in antiviral activity (**14**), but the introduction of axial chirality into the fused bicyclic urazole structure was beneficial to antiviral bioactivity (**9**). In particular, the (*R*)-enantiomers of the axially chiral compounds **9c**, **9f** and **9g** bearing substituted phenyl groups on the dihydropyrazolone fragments possessed excellent anti-PVY activities in both curative and protective effects.

3.4 The result of the expression of PVY-GFP

PVY-GFP agrobacterium infection experiments were carried out to verify the relative antiviral bioactivities of the different enantiomers of the axially chiral compounds **9f** on the curative effects (Fig. 4). The curative effect of (*R*)-**9f** on *N. benthamiana* L. leaves was significantly better than the curative effects of (S)-**9f**, NNM and CK (Control Check). The results clearly demonstrate the critical role played by axial chirality in antiplant virus structures.

3.5 Molecule docking

To get in-depth information on the distinctions between the enantiomers of the axially compounds in their binding abilities to PVY-CP, molecule docking analyses were carried out using Discovery Studio 2020 Client software (Fig. 5). The enantio-enriched

axially chiral compounds (S)-**9h** and (R)-**9h** were initially selected as the target antiviral agents for the molecule docking analysis, since they possessed obvious distinctions in their inactivating activities against PVY. It was found that two conventional hydrogen bonding interactions could be formed between the 3,5-dicarbonyl moiety of (S)-**9h** and the PVY-CP active site of ARG191 at distances of 2.79 Å and 1.94 Å, respectively. Up to nine π -alkyl and alkyl-alkyl interactions could be found between (S)-**9h** and PVY-CP at multiple active sites, such as ALA223, ARG188, MET220 and LEU190. In addition, (S)-**9h** could form a π -cation interaction between the 7-phenyl ring and ARG212 of PVY-CP. All these noncovalent interactions provided (S)-**9h** with strong affinity to PVY-CP, which resulted in effective inactivation of the bioactivity of the virus. In contrast, (R)-**9h** can form two hydrogen bonds with PVY-CP at ARG191, which are weaker than those formed with (S)-**9h**. Moreover, the number of π -alkyl and alkyl-alkyl interactions between (R)-**9h** and PVY-CP were less than its enantiomer (S)-**9h** for steric reasons, therefore (R)-**9h** exhibited a much weaker inactivating activity against PVY than (S)-**9h**.

The enantiomers of compounds (S)-**9f** and (R)-**9f** were also studied in molecule docking since (R)-**9f** showed satisfactory antiviral activities in all curative, protective and inactivating activities against PVY. In this scenario, (S)-**9f** showed only one carbon-hydrogen bond and one π -cation interaction between the chiral molecule and the PVY-CP amino acid sites. In contrast, the (*R*)-enantiomer of **9f** exhibited three hydrogen bonding interactions

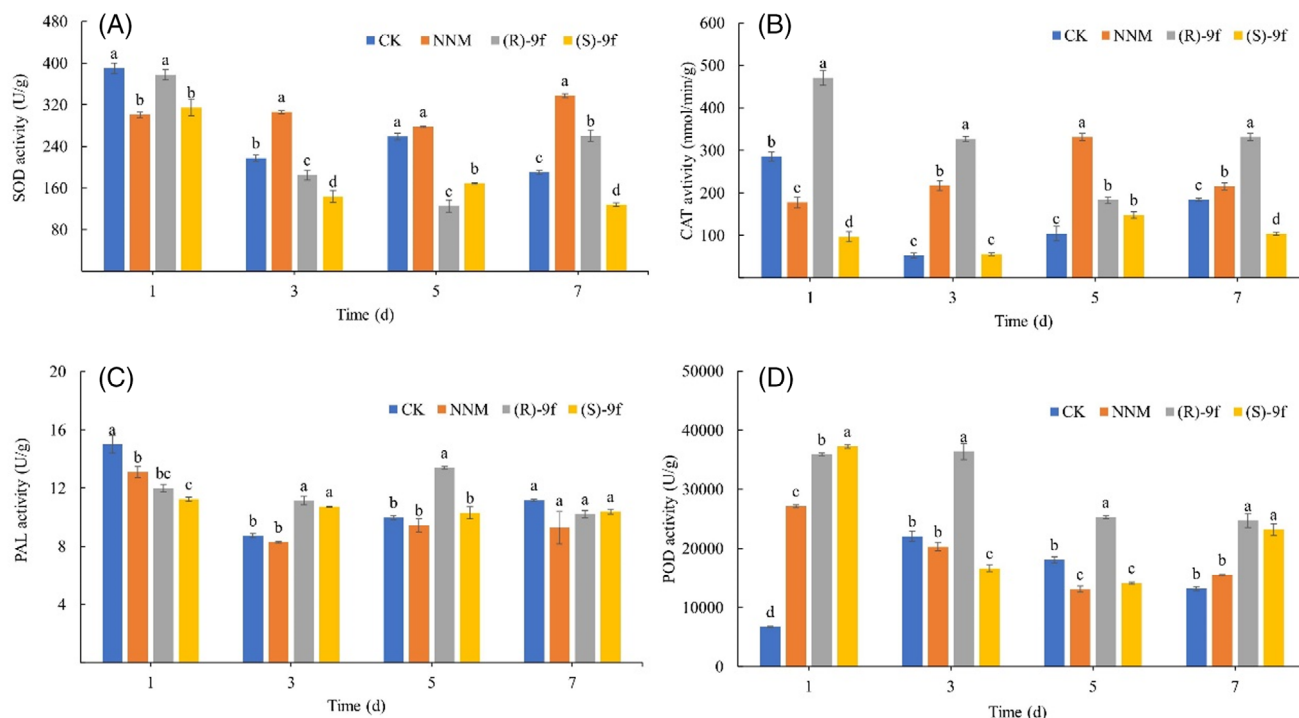


Figure 6. Effect of compound **9f** on defense enzymes from tobacco. (A) Superoxide dismutase (SOD), (B) catalase (CAT), (C) phenylalanine ammonia-lyase (PAL) and (D) peroxidase (POD). Values are the means and standard deviation of three independent experiments. Different lowercase letters indicate values with significant differences among different treatment groups, according to one-way ANOVA ($P < 0.05$).

between the carbonyl groups and the PVY-CP active sites of ARG157 and GLN158. One carbon–hydrogen bonding interaction and up to nine π -alkyl/alkyl–alkyl interactions could also be found within the complex formed from (R)-**9f** and PVY-CP. The molecule docking results were also in accordance with the relative inactivating activities between the (R)- and (S)-enantiomers of **9f**.

3.6 Defensive enzyme activities

The bioactivities of the defensive enzymes SOD, CAT, PAL and POD in tobacco leaves were tested using the antiviral agents of NNM, (S)-**9f** and (R)-**9f** (Fig. 6). The PVY solution was rubbed onto the tobacco leaves 24 h after the leaves had been treated with the antiviral agents. As shown in Fig. 6(a), the bioactivities of the enzyme SOD did not show much difference from the CK group on the first day after inoculation of the virus PVY. SOD activity was suppressed by PVY on the third day after inoculation, although the suppression was alleviated by the antiviral agent NNM. The (R)- and (S)-enantiomers of **9f** showed obvious distinctions in the enhancement of the defense activities of SOD on the seventh day, but both were inferior to NNM. However, the activity of the enzyme CAT was dramatically enhanced by (R)-**9f** throughout the testing period (Fig. 6(b)). The bioactivity of CAT in the tobacco leaves treated with (R)-**9f** was nearly four times higher than (S)-**9f**, and was also higher than NNM on the first, fifth and seventh days after PVY inoculation. The PAL activities of the tobacco leaves treated with the antiviral agents NNM, (S)-**9f** and (R)-**9f** did not show much difference from the CK group throughout the experiments. In contrast, the POD activities were significantly enhanced by all the three antiviral agents, with (R)-**9f** identified as the most effective agent for POD activity promotion during the experimental period. From all the above defense enzyme activity evaluations, we postulate that the outstanding

ability of the axially chiral compound (R)-**9f** in promoting the defense enzyme activities makes a significant contribution to its excellent protective activity against the virus PVY.

4 CONCLUSION

In summary, we have reported the antiplant virus activities of optically pure compounds bearing axial chiralities. Twenty-one groups of axially chiral urazole derivatives bearing (S) and (R) configurations and their racemates were successfully synthesized and evaluated in antiviral activities against the significant plant pathogen PVY. The absolute configurations of the axially chiral compounds exhibited obvious distinctions in antiviral bioactivity, with several of the enantio-enriched axially chiral molecules showing excellent anti-PVY activities. One group of axially chiral compounds (**9f**), with excellent curative and protective activities against PVY, was subjected to mechanistic studies through both molecule docking and defensive enzyme activity tests. Mechanistic studies demonstrated that the axially chiral configurations of the compounds played significant roles in the molecule PVY-CP interactions and could enhance the activities of the defense enzymes. This study provides significant information on the roles that the axial chiralities play in plant protection against plant viruses, paving the way towards the development of novel green pesticides bearing axial chiralities with excellent optical purities.

ACKNOWLEDGEMENTS

We acknowledge funding support from the National Natural Science Foundation of China (32172459, 21961006, 22071036), the Frontiers Science Center for Asymmetric Synthesis and Medicinal Molecules, Department of Education, Guizhou Province

[Qianjiaohe KY number (2020)004], the 10 Talent Plan (Shicengci) of Guizhou Province ([2016]5649), the Science and Technology Department of Guizhou Province ([2018]2802, [2019]1020, Qiankehejichu-ZK[2021]Key033), the Program of Introducing Talents of Discipline to Universities of China (111 Program, D20023) at Guizhou University, the Singapore National Research Foundation under its NRF Investigatorship (NRF-NRFI2016-06) and the Competitive Research Program (NRF-CRP22-2019-0002), and the Ministry of Education, Singapore, under its MOE AcRF Tier 1 Award (RG7/20, RG5/19), MOE AcRF Tier 2 (MOE2019-T2-2-117), and MOE AcRF Tier 3 Award (MOE2018-T3-1-003).

CONFLICT OF INTEREST

No conflict of interest exists in the submission of this manuscript.

DATA AVAILABILITY STATEMENT

The data that supports the findings of this study are available in the supplementary material of this article.

SUPPORTING INFORMATION

Supporting information may be found in the online version of this article.

REFERENCES

- Smith KM, Composite nature of certain potato viruses of the mosaic group. *Nature* **127**:702 (1931).
- Scholthof KB, Adkins S, Czosnek H, Palukaitis P, Jacquot E, Hohn T *et al.*, Top 10 plant viruses in molecular plant pathology. *Mol Plant Pathol* **12**:938–954 (2011).
- Walter CT and Barr JN, Recent advances in the molecular and cellular biology of bunyaviruses. *J Gen Virol* **92**:2467–2484 (2011).
- Wylie SJ, Adams M, Chalam C, Kreuze J, López-Moya JJ, Ohshima K *et al.*, ICTV virus taxonomy profile: Potyviridae. *J Gen Virol* **98**:352–354 (2017).
- Kezar A, Kavcic L, Polak M, Novacek J, Gutierrez-Aguirre I, Znidaric MT *et al.*, Structural basis for the multitasking nature of the potato virus Y coat protein. *Sci Adv* **5**:eaaw3808 (2019).
- Smith KM, Studies on the spread of certain plant viruses in the field. *Ann Appl Biol* **30**:345–348 (1943).
- Kennedy JS, Aphid migration and the spread of plant viruses. *Nature* **165**:1024–1025 (1950).
- Chen Y, Chen Q, Li M, Mao Q, Chen H, Wu W *et al.*, Autophagy pathway induced by a plant virus facilitates viral spread and transmission by its insect vector. *PLoS Pathog* **13**:e1006727 (2017).
- Zhao L, Feng C, Wu K, Chen W, Chen Y, Hao X *et al.*, Advances and prospects in biogenic substances against plant virus: a review. *Pestic Biochem Physiol* **135**:15–26 (2017).
- Zhang S, Griffiths JS, Marchand G, Bernards MA and Wang A, Tomato brown rugose fruit virus: an emerging and rapidly spreading plant RNA virus that threatens tomato production worldwide. *Mol Plant Pathol* **23**:1262–1277 (2022).
- Dupuis B, The movement of potato virus Y (PVY) in the vascular system of potato plants. *Eur J Plant Pathol* **147**:365–373 (2017).
- Onditi J, Nyongesa M and van der Vlugt R, Screening for PVYN-Wi resistance in Kenyan potato cultivars. *Potato Res* **64**:469–488 (2021).
- Gildemacher PR, Demo P, Barker I, Kaguongo W, Woldegiorgis G, Wagoire WW *et al.*, A description of seed potato systems in Kenya, Uganda and Ethiopia. *Am J Potato Res* **86**:373–382 (2009).
- Zhang J, Zhao L, Zhu C, Wu Z, Zhang G, Gan X *et al.*, Facile synthesis of novel vanillin derivatives incorporating a bis(2-hydroxyethyl)dithioacetal moiety as antiviral agents. *J Agric Food Chem* **65**:4582–4588 (2017).
- Wei C, Zhang J, Shi J, Gan X, Hu D and Song B, Synthesis, antiviral activity, and induction of plant resistance of indole analogues bearing dithioacetal moiety. *J Agric Food Chem* **67**:13882–13891 (2019).
- Ulrich EM, Morrison CN, Goldsmith MR and Foreman WT, Chiral pesticides: Identification, description, and environmental implications. *Rev Environ Contam Toxicol* **217**:1–74 (2012).
- Chen T, Xiong H, Yang JF, Zhu XL, Qu RY and Yang GF, Diaryl ether: a privileged scaffold for drug and agrochemical discovery. *J Agric Food Chem* **68**:9839–9877 (2020).
- Zheng Z, Dai A, Jin Z, Chi YR and Wu J, Trifluoromethylpyridine: an important active fragment for the discovery of new pesticides. *J Agric Food Chem* **70**:11019–11030 (2022).
- Zhang Q, Xiong W, Gao B, Cryder Z, Zhang Z, Tian M *et al.*, Enantioselectivity in degradation and ecological risk of the chiral pesticide ethiprole. *Land Degrad Dev* **29**:4242–4251 (2018).
- Chang W, Nie J and Yan Z, Enantioselective behavior of chiral difenocnazole in apple and field soil. *Bull Environ Contam Toxicol* **103**:501–505 (2019).
- Anjos CS, Lima RN and Porto ALM, An overview of neonicotinoids: biotransformation and biodegradation by microbiological processes. *Environ Sci Pollut Res* **28**:37082–37109 (2021).
- Arenas M, Martín J, Santos JL, Aparicio I and Alonso E, Enantioselective behavior of environmental chiral pollutants: a comprehensive review. *Crit Rev Environ Sci Technol* **52**:2995–3034 (2021).
- Ribeiro C, Gonçalves R and Tiritan ME, Separation of enantiomers using gas chromatography: application in forensic toxicology, food and environmental analysis. *Crit Rev Anal Chem* **51**:787–811 (2021).
- Yang G, Liu Z, Lan T, Dou L and Zhang K, Potential enantioselectivity of the hydrolysis and photolysis of the chiral agrochemical penthiopyrad in aquatic environments. *Environ Sci: Water Res Technol* **7**:1220–1229 (2021).
- Santos AR, Pinheiro AC, Sodero ACR, Cunha AS, Padilha MC, Sousa PM *et al.*, Atropoisomerismo: O efeito da quiralidade axial em substâncias bioativas. *Quim Nova* **30**:125–135 (2007).
- LaPlante SR, Edwards PJ, Fader LD, Jakalian A and Huckle O, Revealing atropisomer axial chirality in drug discovery. *ChemMedChem* **6**:505–513 (2011).
- Zask A, Murphy J and Ellestad GA, Biological stereoselectivity of atropisomeric natural products and drugs. *Chirality* **25**:265–274 (2013).
- Gustafson J, Nalbandian C and Hecht D, The preorganization of atropisomers to increase target selectivity. *Synlett* **27**:977–983 (2016).
- Glunz PW, Recent encounters with atropisomerism in drug discovery. *Bioorg Med Chem Lett* **28**:53–60 (2018).
- Toenjes ST and Gustafson JL, Atropisomerism in medicinal chemistry: challenges and opportunities. *Future Med Chem* **10**:409–422 (2018).
- Mancinelli M, Bencivenni G, Pecorari D and Mazzanti A, Stereochemistry and recent applications of axially chiral organic molecules. *Eur J Org Chem* **2020**:4070–4086 (2020).
- Chen S, Zhang L, Chen H, Chen Z and Wen Y, Enantioselective toxicity of chiral herbicide metolachlor to *microcystis aeruginosa*. *J Agric Food Chem* **67**:1631–1637 (2019).
- Muller MD, Poiger T and Buser H, Isolation and identification of the metolachlor stereoisomers using high-performance liquid chromatography, polarimetric measurements, and enantioselective gas chromatography. *J Agric Food Chem* **49**:42–49 (2001).
- Liu Y, Zhang X, Liu C, Yang R, Xu Z, Zhou L *et al.*, Enantioselective and synergistic toxicity of axial chiral herbicide propisochlor to SP2/0 myeloma cells. *J Agric Food Chem* **63**:7914–7920 (2015).
- Bringmann G, Price Mortimer AJ, Keller PA, Gresser MJ, Garner J and Breuning M, Atroposelective synthesis of axially chiral biaryl compounds. *Angew Chem Int Ed* **44**:5384–5427 (2005).
- Brandes S, Niess B, Bella M, Prieto A, Overgaard J and Jorgensen KA, Non-biaryl atropisomers in organocatalysis. *Chemistry* **12**:6039–6052 (2006).
- Tanaka K, Takeishi K and Noguchi K, Enantioselective synthesis of axially chiral anilides through rhodium-catalyzed [2+2+2] cycloaddition of 1,6-diyne with trimethylsilylynamides. *J Am Chem Soc* **128**:4586–4587 (2006).
- Wencel-Delord J, Panossian A, Leroux FR and Colobert F, Recent advances and new concepts for the synthesis of axially stereo-enriched biaryls. *Chem Soc Rev* **44**:3418–3430 (2015).
- Bonne D and Rodriguez J, Enantioselective syntheses of atropisomers featuring a five-membered ring. *Chem Commun* **53**:12385–12393 (2017).
- Hasegawa F, Kawamura K, Tsuchikawa H and Murata M, Stable C-N axial chirality in 1-aryluracil scaffold and differences in *in vitro* metabolic clearance between atropisomers of PDE4 inhibitor. *Bioorg Med Chem* **25**:4506–4511 (2017).

- 41 Bonne D and Rodriguez J, A bird's eye view of atropisomers featuring a five-membered ring. *Eur J Org Chem* **2018**:2417–2431 (2018).
- 42 Li SL, Yang C, Wu Q, Zheng HL, Li X and Cheng JP, Atroposelective catalytic asymmetric allylic alkylation reaction for axially chiral anilides with achiral Morita-Baylis-Hillman carbonates. *J Am Chem Soc* **140**: 12836–12843 (2018).
- 43 Zilate B, Castrogiovanni A and Sparr C, Catalyst-controlled stereoselective synthesis of atropisomers. *ACS Catal* **8**:2981–2988 (2018).
- 44 Lu S, Ng SVH, Lovato K, Ong JY, Poh SB, Ng XQ *et al.*, Practical access to axially chiral sulfonamides and biaryl amino phenols via organocatalytic atroposelective *N*-alkylation. *Nat Commun* **10**:3061 (2019).
- 45 Bao X, Rodriguez J and Bonne D, Enantioselective synthesis of atropisomers with multiple stereogenic axes. *Angew Chem Int Ed* **59**: 12623–12634 (2020).
- 46 Bertuzzi G and Corti V, Organocatalytic asymmetric methodologies towards the synthesis of atropisomeric *N*-heterocycles. *Synthesis* **52**:2450–2468 (2020).
- 47 Dong Y, Liu R and Wang W, Catalytic asymmetric catellani-type reaction: a powerful tool for axial chirality construction. *Green Synth Catal* **1**:83–85 (2020).
- 48 Ong JY, Ng XQ, Lu S and Zhao Y, Isothiourea-catalyzed atroposelective *N*-acylation of sulfonamides. *Org Lett* **22**:6447–6451 (2020).
- 49 Yang G-H, Zheng H, Li X and Cheng J-P, Asymmetric synthesis of axially chiral phosphamides via atroposelective allylic alkylation. *ACS Catal* **10**:2324–2333 (2020).
- 50 Hall IH, Simlot R, Day P, Wong OT, ElSourady H and Izydore RA, The hypolipidemic effects of 1-acetyl-4-phenyl-1,2,4-triazolidine-3,5-dione in rodents. *Pharm Res* **10**:1206–1211 (1993).
- 51 Martinez A, Alonso M, Castro A, Dorronsoro I, Gelpi JL, Luque FJ *et al.*, Sar and 3D-QSAR studies on thiadiazolidinone derivatives: exploration of structural requirements for glycogen synthase kinase 3 inhibitors. *J Med Chem* **48**:7103–7112 (2005).
- 52 Adibi H, Abiri R, Mallakpour S, Zolfigol MA and Majnooni MB, Evaluation of in vitro antimicrobial and antioxidant activities of 4-substituted-1,2,4-triazolidine-3,5-dione derivatives. *J Rep Pharm Sci* **1**:87–93 (2012).
- 53 Saluja P, Khurana JM, Nikhil K and Roy P, Task-specific ionic liquid catalyzed synthesis of novel naphthoquinone–urazole hybrids and evaluation of their antioxidant and *in vitro* anticancer activity. *RSC Adv* **4**:34594–34603 (2014).
- 54 Saluja P, Khurana JM, Sharma C and Aneja KR, An efficient and convenient approach for the synthesis of novel pyrazolo[1,2-*a*]triazoletriones and evaluation of their antimicrobial activities. *Aust J Chem* **67**:867–874 (2014).
- 55 Pelit E, Oikonomou K, Gul M, Georgiou D, Szafert S, Katsamakas S *et al.*, α -amination and the 5-exo-trig cyclization reaction of sulfur-containing schiff bases with *N*-phenyltriazolinedione and their anti-lipid peroxidation activity. *C R Chim* **20**:424–434 (2017).
- 56 Varmaghani F, Hassan M, Nematollahi D and Mallakpour S, Electrochemical synthesis of diverse sulfonamide derivatives depending on the potential electrode and their antimicrobial activity evaluation. *New J Chem* **41**:8279–8288 (2017).
- 57 Llabani E, Hicklin RW, Lee HY, Motika SE, Crawford LA, Weerapana E *et al.*, Diverse compounds from pleuromutilin lead to a thioredoxin inhibitor and inducer of ferroptosis. *Nat Chem* **11**:521–532 (2019).
- 58 Xin X, Zimmermann S, Flegel J, Otte F, Knauer L, Strohmman C *et al.*, Unravelling the synthesis and chemistry of stable, acyclic, and double-deficient 1,3-butadienes: an endo-selective Diels-Alder route to hedgehog pathway inhibitors. *Chem Eur J* **25**:2717–2722 (2019).